pH-dependent domain formation in phosphatidylinositol polyphosphate/phosphatidylcholine mixed vesicles

Duane A. Redfern and Arne Gericke[1]

Chemistry Department, Kent State University, Kent, OH 44242

Abstract **Phosphatidylinositol polyphosphates (PI-PPs) have been shown to mediate a large variety of physiological processes by attracting proteins to specific cellular sites. Such site-specific signaling requires local accumulation of PI-PPs, and in light of the rich headgroup functionality, it is conceivable that hydrogen bond formation between adjacent headgroups is a contributing factor to the formation of PI-PP-enriched domains. To explore the significance of hydrogen bond formation for the mutual interaction of PI-PPs, this study aims to characterize the pH-dependent phase behavior of phosphatidylcholine/phosphatidylinositol bisphosphate and trisphosphate mixed vesicles by differential scanning calorimetry, infrared transmission spectroscopy, and fluorescence resonance energy transfer measurements. For pH values >7–7.5, the experiments yielded results consistent with dipalmitoylphosphatidylcholine/dipalmitoylphosphatidylinositol polyphosphate gel phase demixing, whereas for moderately acidic conditions, an enhanced mixing was observed. Similarly, this pH-dependent formation of PI-PP-enriched domains was also found for the physiologically important fluid phase. The stability of PI-PP-enriched domains and to some extent the pH dependence of the domain formation was governed by the number as well as the position of the phosphomonoester groups at the inositol ring.—**Redfern, D. A., and A. Gericke. **pH-dependent domain formation in phosphatidylinositol polyphosphate/phosphatidylcholine mixed vesicles. *J. Lipid Res.* 2005.** 46: **504–515.**

Supplementary key words phosphoinositide • lipid demixing • calorimetry • infrared • fluorescence

Phosphoinositides (**Fig. 1**) have been shown to control membrane trafficking events by recruiting proteins to specific cellular sites (1, 2). The temporal control of phosphoinositide-mediated signaling events is facilitated by a broad range of kinases and phosphatases (1, 3), whereas the signaling specificity is rooted in selective protein binding as well as a high degree of phosphoinositide compartmentalization. This compartmentalization is not only evident in the accumulation of distinct phosphoinositide derivatives in particular cell entities [e.g., enrichment of phosphatidylinositol-3-phosphate in early endosomes and phosphatidylinositol-4-phosphate in the Golgi (2, 4–6)] but manifests itself also in the formation of phosphoinositide-enriched domains. Several studies have reported the raft-dependent (7–13) and raft-independent (14–17) accumulation of phosphoinositides in vivo; however, the mechanisms that lead to such phosphoinositide segregation are elusive. For example, the recruitment of certain phosphoinositides to raft domains raises the question of what kind of molecular interactions and physiological conditions aid such targeting, which is generally unfavorable for lipids with unsaturated acyl chains (the typical chain composition of phosphoinositides is stearoyl/arachidonoyl). Simple lipid partitioning models cannot explain phosphoinositide enrichment in rafts, because measurements on monolayer systems failed to show any phosphatidylinositol-4,5-bisphosphate (PI-4,5-P_2) accumulation in cholesterol-enriched domains (although such studies have some limitations when compared with bilayer systems) (18).

Manuscript received 24 September 2004 and in revised form 2 December 2004.

Published, JLR Papers in Press, December 16, 2004.
DOI 10.1194/jlr.M400367-JLR200

Abbreviations: Bodipy-PI-3,4-P_2, D(+)-*sn*-1-*O*-[1-[6′-[6-[((4-(4,4-difluoro-5-(2-thienyl)-4-bora-3a,4a-diaza-*s*-indacene-3-yl)phenoxy)acetyl)amino]hexanoyl]amino]hexanoyl]2-hexanoylglyceryl D-*myo*-phosphatidylinositol-3,4-bisphosphate; Bodipy TR, [1-[6′-[6-[((4-(4,4-difluoro-5-(2-thienyl)-4-bora-3a,4a-diaza-*s*-indacene-3-yl)phenoxy)acetyl)amino]hexanoyl]amino]hexanoyl]; Bodipy TMR, [1-[6′-[6-[(4,4-difluoro-1,3-dimethyl-5-(4-methoxyphenyl)-4-bora-3a,4a-diaza-*s*-indacene-2-propionoyl)amino]hexanoyl]amino]hexanoyl]; CHES, 2-[N-cyclohexylamino]ethanesulfonic acid; DPPC, dipalmitoylphosphatidylcholine; DPPI, dipalmitoylphosphatidylinositol; DPPI-3,4-P_2, dipalmitoylphosphatidylinositol-3,4-bisphosphate; DPPI-3,5-P_2, dipalmitoylphosphatidylinositol-3,5-bisphosphate; DPPI-3,4,5-P_3, dipalmitoylphosphatidylinositol-3,4,5-trisphosphate; DPPI-4,5-P_2, dipalmitoylphosphatidylinositol-4,5-bisphosphate; DSC, differential scanning calorimetry; FRET, fluorescence resonance energy transfer; FTIR, Fourier transform infrared; MARCKS, myristoylated alanine-rich C kinase substrate; NBD-PC, 1-palmitoyl-2-[12-[(7-nitro-2-1,3-benzoxadiazol-4-yl)amino]dodecanoyl]*sn*-glycero-3-phosphocholine; PA, phosphatidic acid; PC, phosphatidylcholine; PI-3,4-P_2, phosphatidylinositol-3,4-bisphosphate; PI-3,4,5-P_3, phosphatidylinositol-3,4,5-trisphosphate; PI-3,5-P_2, phosphatidylinositol-3,5-bisphosphate; PI-4,5-P_2, phosphatidylinositol-4,5-bisphosphate; PI-PP, phosphatidylinositol polyphosphate; PI-xP, phosphatidylinositol monophosphate; POPC, palmitoyloleoylphosphatidylcholine; SAPI-3,4,5-P_3, stearoylarachidonoylphosphatidylinositol-3,4,5-trisphosphate; T_m, melting temperature; $\nu_a(CD_2)$, antisymmetric CD_2 stretching vibration band; $\nu_s(CH_2)$, symmetric CH_2 stretching band.

[1] To whom the correspondence should be addressed.
e-mail agericke@kent.edu

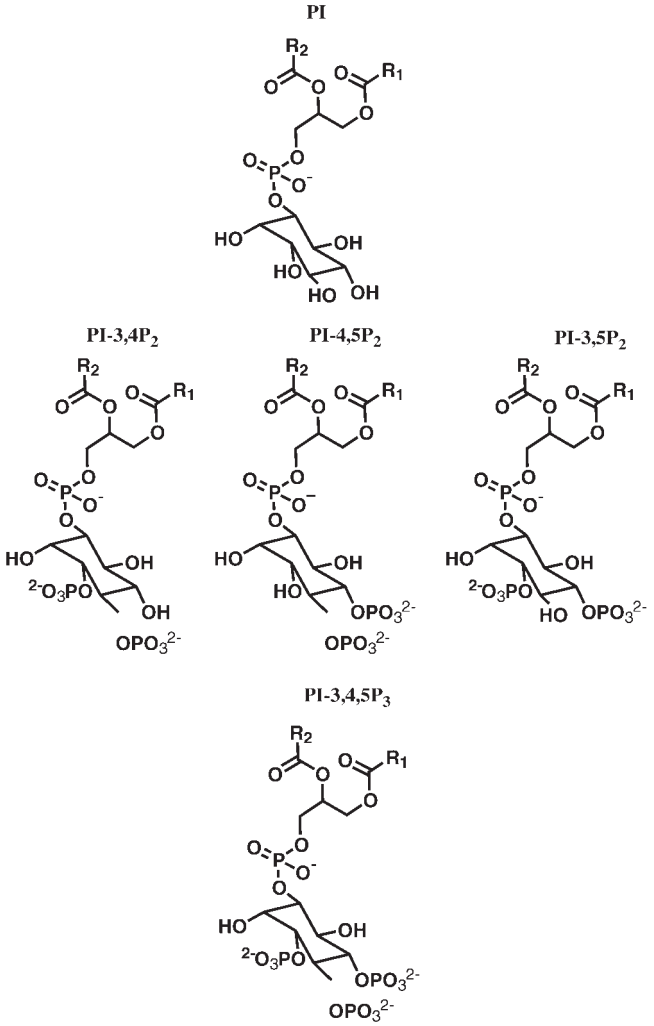

Fig. 1. Chemical structures of phosphatidylinositol (PI), phosphatidylinositol-3,4-phosphate (PI-3,4-P_2), phosphatidylinositol-4,5-phosphate (PI-4,5-P_2), phosphatidylinositol-3,5-phosphate (PI-3,5-P_2), and phosphatidylinositol-3,4,5-phosphate (PI-3,4,5-P_3).

It was suggested that the site-specific recruitment of phosphoinositide kinases and the resulting localized production of distinct phosphoinositides leads to the formation of phosphoinositide-enriched domains (16), which is a notion supported by a number of studies demonstrating the colocalization of phosphoinositide kinases and raft domain markers (7, 9, 19, 20). Although localized production is certainly a contributing factor, it alone cannot explain phosphoinositide enrichment, because diffusion away from the site of synthesis will most likely limit the accumulation. It has been shown that protein motifs rich in cationic amino acid residues [e.g., the myristoylated alanine-rich C kinase substrate (MARCKS) effector domain (4, 11, 18, 21)] aid the formation of PI-4,5-P_2-enriched domains. MARCKS/PI-4,5-P_2 binding has been shown to be cholesterol independent; however, the NAP22/PI-4,5-P_2 interaction has been found to be strongly influenced by the presence of cholesterol (22). Although protein-induced phosphoinositide sequestration is certainly a major factor in the local accumulation of these lipids, it is likely that phosphoinositide domain formation depends on several factors. In light of the rich functionality of the phosphoinositide headgroup, it is conceivable that mutual interaction via hydrogen bond formation is a contributing factor to the formation of phosphoinositide-enriched domains.

In a recent study on phosphatidylinositol monophosphate (PI-xP)/phosphatidylcholine (PC) mixed vesicles (23), our laboratory has shown that the mutual interaction of PI-xPs is increased for pH values of >7.0. This pH-dependent interaction resulted not only in PI-xP/PC gel phase demixing but also yielded the formation of PI-xP-enriched domains in the fluid phase at high pH. The enhanced PI-xP interaction at high pH is markedly different from the behavior found for phosphatidic acid (PA), which also exhibits a phosphomonoester group in its headgroup. In the case of PA, maximum mutual interaction was observed between the Pk_{a1} and Pk_{a2} of the phosphomonoester group, which was attributed to the formation of a hydrogen bond network between adjacent phosphomonoester groups (i.e., the phosphomonoester groups function as hydrogen donors as well as hydrogen acceptors). For PI-xPs, maximum mutual interaction was observed for pH values associated with a predominantly deprotonated phosphomonoester group, which rules out a hydrogen-donating function of this functional group. However, comparison with phosphatidylinositol (PI) revealed a stronger stabilization of PI-xP-enriched phases, which suggests that the phosphomonoester group contributes to the mutual interaction by accepting hydrogens from nearby hydroxyl groups.

This report extends the previous study (23) to phosphatidylinositol polyphosphates (PI-PPs), namely phosphatidylinositol-3,4-bisphosphate (PI-3,4-P_2), phosphatidylinositol-3,5-bisphosphate (PI-3,5-P_2), PI-4,5-P_2, and phosphatidylinositol-3,4,5-trisphosphate (PI-3,4,5-P_3). The experiments were designed to explore the importance of hydrogen bond formation for the mutual interaction of PI-PPs and to investigate whether the position of the phosphomonoester groups at the inositol ring affects the physicochemical properties of the respective phosphoinositide. Compared with PI-xPs, PI-PPs exhibit higher headgroup charges, which are expected to lead to an enhanced electrostatic repulsion. On the other hand, the increased number of phosphomonoester groups results in more sites for hydrogen bond formation, which might compensate for the unfavorable repulsive forces. Differential scanning calorimetry (DSC) and temperature-dependent infrared transmission spectroscopy were used to study the gel phase miscibility of mixed multilamellar dipalmitoylphosphatidylinositol (DPPI) polyphosphate/dipalmitoylphosphatidylcholine (DPPC) vesicles. These pH-dependent measurements shed light on the importance of hydrogen bond formation for the mutual phosphoinositide interaction and provide information about the relative stabilities of phosphoinositide-enriched domains. It turns out that the results from these measurements are indicative of a pH-dependent gel phase immiscibility, which raises the question of whether this immiscibility translates into domain formation in fluid PI-PP/PC phases. To address this question, a recently developed flu-

orescence resonance energy transfer (FRET) protocol was used, which enables the pH-dependent analysis of PI-PP/PC mixing behavior. The FRET measurements furnished results consistent with the formation of fluid PI-PP-enriched domains at high pH (depending of the nature of the phosphoinositide pH > 7.0–7.5), whereas pH reduction resulted in an enhanced mixing of the two lipid components.

MATERIALS AND METHODS

Materials

DPPI-3,4-bisphosphate (DPPI-3,4-P_2), DPPI-4,5-bisphosphate (DPPI-4,5-P_2), DPPI-3,4,5-trisphosphate (DPPI-3,4,5-P_3), and stearoylarachidonoylphosphatidylinositol-3,4,5-trisphosphate (SAPI-3,4,5-P_3) were obtained from Cayman Chemical (Ann Arbor, MI; >98% purity). DPPI-3,5-bisphosphate (DPPI-3,5-P_2) was obtained from A. G. Scientific (San Diego, CA; 99% purity). DPPC, 1-palmitoyl-2-oleoylphosphatidylcholine (POPC), brain phosphatidylinositol-4-phosphate, brain PI-4,5-P_2, bovine liver phosphatidylinositol, and acyl chain perdeuterated dipalmitoylphosphatidylcholine-d_{62} (DPPC-d_{62}) were obtained from Avanti Polar Lipids (Alabaster, AL; the purity of the synthetic lipids was 99%). All lipids in this study were used as received. Fluorescently labeled D(+)-*sn*-1-*O*-[1-[6′-[6-[((4-(4,4-difluoro-5-(2-thienyl)-4-bora-3a,4a-diaza-*s*-indacene-3-yl)phenoxy)acetyl)amino]hexanoyl]amino]hexanoyl] 2-hexanoylglyceryl D-*myo*-phosphatidylinositol-3,4-bisphosphate (Bodipy-PI-3,4-P_2; excitation, 589 nm; emission, 617 nm) as well as the corresponding Bodipy-PI-4,5-P_2 and Bodipy-PI-3,5-P_2 were obtained from Molecular Probes (Eugene, OR; >95% purity). Chain-labeled 1-palmitoyl-2-[12-[(7-nitro-2-1,3-benzoxadiazol-4-yl)amino] dodecanoyl]*sn*-glycero-3-phosphocholine (NBD-PC; excitation, 460 nm; emission, 534 nm) was obtained from Avanti Polar Lipids. All buffers (HEPES, MES, 2-[N-cyclohexylamino]ethanesulfonic acid (CHES), and sodium citrate) as well as EDTA and NaCl were of enzyme-grade purity (Fisher Scientific, Chicago, IL). Buffers had the general composition 100 mM NaCl, 10 mM buffer, and 0.1 mM EDTA and were adjusted to the appropriate pH using aqueous HCl or NaOH. The buffers were used as follows: pH 9.5, CHES; pH 8.5 and 7.4, HEPES; pH 6.5 and 5.5, MES; pH 4.5, sodium citrate. Chloroform and methanol, which were used to prepare lipid stock solutions, were American Chemical Society (ACS) grade, and the water used for buffer preparation was HPLC grade (all from Fisher Scientific).

Sample preparation

Lipids were stored in chloroform-methanol (2:1) stock solutions. In the case of phosphoinositides, small amounts of water were added to the organic solvent mixture. Mixed multilamellar vesicles were prepared by drying appropriate amounts of the stock solutions in a stream of dry nitrogen. To avoid lipid demixing attributable to solubility differences among the components of the lipid mixture (which has been shown in some instances to affect the mixing properties in the formed vesicles), this drying process was carried out as quickly as possible at slightly increased temperatures (~50°C). Subsequently, the samples were kept overnight in high vacuum at 45°C. The lipid mixtures were resuspended in the appropriate buffer solution, heated for 5–10 min to ~50°C, and vortexed for 60 s. This heating/vortexing procedure was repeated two more times. For the DSC and infrared measurements, these lipid suspensions were used for the measurement. The final total lipid concentrations were 0.3 mM for the DSC experiments and 40.6 mM (lipid-water ratio 1:30, w/w) for the Fourier transform infrared (FTIR) measurements. For the fluorescence measurements, unilamellar vesicles were obtained by extruding the multilamellar vesicles at either ~70°C (saturated acyl chain lipids) or ~40°C (naturally occurring acyl chain composition) through a 100 nm pore size membrane (Avestin, Ottawa, Ontario, Canada). The quality of the extrusion was checked regularly by dynamic light scattering [High Performance Particle Sizer (HPPS); Malvern Instruments, Southborough, MA]. Typically, a narrow intensity distribution that was centered at a 110–130 nm vesicle diameter was obtained. The lipid concentration used for the fluorescence experiments was similar to the DSC measurement concentrations, 0.18 mM.

DSC

DSC measurements of mixed multilamellar vesicles were carried out using a Microcal VP-DSC (Northampton, MA). The scan rate was 0.5°C/min, and the total lipid concentration was 0.3 mM. A total of six heating/cooling scans (4–90°C) were recorded, and the third heating scan (the fifth scan overall) was usually found to be representative (the second, third, fourth, fifth, and sixth heating scans were essentially the same).

FTIR transmission spectroscopy

FTIR experiments were carried out with a Tensor 27 spectrometer (Bruker, Billerica, MA) equipped with a broad-band Mercury Cadmium Tellur (MCT) detector. Interferograms were collected at 4 cm^{-1} resolution (500 scans), apodized with a Blackman-Harris function, and Fourier transformed with two levels of zero filling to yield spectra encoded at 1 cm^{-1} intervals. Lipid samples (40.6 mM) were sandwiched between two BaF_2 windows [25 μm polytetrafluoroethylene (PTFE) spacer] and placed in a Wilmad (Buena, NJ) temperature-controlled liquid cell holder. The sample temperature was monitored using a thermocouple attached to an Omega (Stamford, CT) DP 116 thermometer (0.1°C relative accuracy). The sample temperature was adjusted using a computer-controlled thermostated water bath. The temperature-dependent acquisition of infrared spectra between 4°C and 90°C took ~30 h. The samples were checked for proper hydration by visual inspection and by monitoring the water-stretching band intensities. The spectra were processed using the software supplied by the instrument manufacturer. The positions of the methylene-stretching vibration bands were determined by calculating the second derivative followed by a center-of-mass peak pick algorithm. This typically results in a peak position accuracy of ±0.1 cm^{-1}.

FRET measurements

Fluorescence measurements were carried out using a Cary Eclipse fluorescence spectrometer (Varian, Walnut Creek, CA) equipped with a temperature-controlled sample holder. Unilamellar mixed vesicles (0.18 mM total lipid, 15% PI-PP/85% PC) were made as described above, and subsequently, aqueous buffer dispersions of the fluorescently labeled lipids were added to the preformed unilamellar vesicles. The samples were kept for at least 1 h at a temperature above the melting transition of the respective lipid mixtures (i.e., 70°C for saturated lipids, 20°C for unsaturated lipids). The insertion of the fluorescent lipids into the outer leaflet of the bilayer was monitored based upon the NBD-PC emission intensity (the NBD dye is nonfluorescent in an aqueous medium), which reached steady state ~60 min after the addition of the labeled lipids. The concentration of the respective NBD lipid was 1% of the total lipid concentration, whereas the concentration of the Bodipy lipid was 1.2%. These concentrations were determined to be optimal for a minimal transfer in the demixed state

and a maximum resonance energy transfer in the mixed lipid state. The [1-[6'-[6-[((4-(4,4-difluoro-5-(2-thienyl)-4-bora-3a,4a-diaza-s-indacene-3-yl)phenoxy)acetyl)amino]hexanoyl]amino]hexanoyl] (Bodipy-TR) fluorophore (excitation, 589 nm; emission, 617 nm) used for this investigation is not the best FRET partner for the NBD fluorophore (excitation, 460 nm; emission, 534 nm). At first glance, [1-[6'-[6-[(4,4-difluoro-1,3-dimethyl-5-(4-methoxyphenyl)-4-bora-3a,4a-diaza-s-indacene-2-propionoyl)amino]hexanoyl]amino]hexanoyl] (Bodipy-TMR) (excitation, 542 nm; emission, 574 nm) appears to be better suited for an NBD donor because of the more favorable position of the absorption band. However, a closer inspection of the Bodipy-TMR absorption spectrum revealed a significant direct excitation of the Bodipy fluorophore for an excitation wavelength between 440 and 460 nm. In contrast, Bodipy-TR shows almost no direct excitation at this wavelength. For all FRET experiments, an excitation wavelength of 440 nm was used. The labeled unilamellar vesicles were titrated with 0.1 N HCl from a high to a low pH value. After each titration step, samples were allowed to equilibrate for at least 6 min (longer waiting times did not lead to deviating results). The observed mixing properties of the respective lipid mixtures were completely reversible (i.e., adjustment of the pH back to ~10 at the end of the experiment resulted in resonance energy transfer ratios similar to those obtained at the beginning of the titration). The integrity of the vesicles was routinely checked by dynamic light scattering after completion of the titrations, and no vesicle fusion or decomposition was detectable.

RESULTS

DSC

Phosphoinositides usually form in aqueous solution, depending on pH and salt concentration, micellar or nonlamellar phases (24). Therefore, single-component phosphatidylinositol bisphosphate and trisphosphate systems are not suitable as models for biological membranes; instead, phosphoinositide/lipid mixtures have to be used. We have investigated the thermotropic behavior of mixed DPPI-x,y-P_2/DPPC (15:85) multilamellar vesicles for pH values between 5.5 and 9.5 (**Fig. 2**). In Fig. 2A, DSC thermograms for different DPPI-x,y-P_2/PC mixtures are shown as a function of pH, and in Fig. 2B, the corresponding thermograms for DPPI-3,4,5-P_3/DPPC mixed vesicles are displayed. For all investigated mixed vesicle systems, the DPPC pretransition peak is abolished, the main phase transition is broadened (indicating reduced cooperativity), and the phase transition temperature increases as the pH is decreased. However, a more detailed comparison of the thermotropic behavior of the different phosphatidylinositol bisphosphate and trisphosphate/DPPC mixtures reveals significant differences. For the DPPI-3,4-P_2-containing mixtures, the main phase transition peak is split for intermediate pH values, whereas at pH 9.5, this splitting is reduced and the phase transition temperature is lowest. For pH 5.5, the main transition peak is broadened, shifted to a higher temperature, and a small shoulder is discernible above the melting temperature (T_m) of pure DPPC (marked by a line). For DPPI-3,5-P_2/DPPC mixtures, a broad shoulder at high temperatures develops as the pH is being decreased. This broad high-temperature shoulder, which is already discernible at pH 8.5, is a unique feature of the DPPI-3,5-P_2/DPPC system and is not found for any of the other phosphoinositide/DPPC mixtures (Fig. 2). In the case of the DPPI-4,5-P_2/DPPC mixtures, the phase transition shifts to a higher temperature as the pH is being decreased, mainly because a low-temperature component at 39°C decreases in intensity, whereas a high-temperature component becomes more dominant. Similarly, the DSC peak for DPPI-3,4,5-P_3/DPPC mixtures evolves from a narrow peak located at 39.0°C to a broad transition peak centered at ~41.1°C. Generally, all DSC experiments showed a good reversibility (i.e., repeated heating scans matched very well), and only a small hysteresis (difference of the T_m values for heating and cooling scans) was found. Furthermore, slower scan rates (0.25°C/min) did not alter the results (data not shown).

For mixed lipid vesicles with low concentrations of the minority component (<20%), it was shown recently that the phase transition peak in the DSC thermogram is largely associated with the majority component. As a result, even in a completely demixed state, the phase behavior of the minority component is often elusive (particularly for broad transitions) (25). This implies for the data presented above that the transition peaks observed in the DSC thermograms are largely linked to the thermotropic behavior of DPPC-rich phases (i.e., a broadening or shift of the DSC peak can be attributed to DPPC being in environments with varying amounts of phosphoinositides). In addition, a phase transition peak with components significantly above the T_m of pure DPPC, as observed for DPPI-3,5-P_2/DPPC mixed vesicles at pH $\leq$ 7.4, indicates nonideal mixing with favored interactions between unlike molecules, which results in a stabilization of the DPPC-rich phase as marked by the higher T_m (although this could be conclusively answered only by investigating the entire DPPI-3,5-P_2/DPPC phase diagram, which is not possible because pure phosphoinositide vesicles cannot be fabricated).

Compared with DPPI-xP/DPPC mixed vesicles (23), the phase transition peaks for phosphatidylinositol bisphosphate- and trisphosphate-containing mixtures are generally broader (less cooperative) and shift more significantly to higher temperatures as the pH is decreased. Differences in the phase behavior of the respective mixed vesicles are not only observed for varying numbers of phosphomonoester groups at the inositol ring of the phosphoinositide component but are also linked to the phosphomonoester position at the inositol ring. Although deviations in phase behavior were also found among DPPI-xP/DPPC mixtures, they are much more pronounced among DPPI-x,y-P_2-containing mixed vesicles (Fig. 2A).

As mentioned above, the phase transitions of the respective phosphoinositide components are elusive, which can be attributed to the broad nature of the transition and the low phosphoinositide concentrations used in the

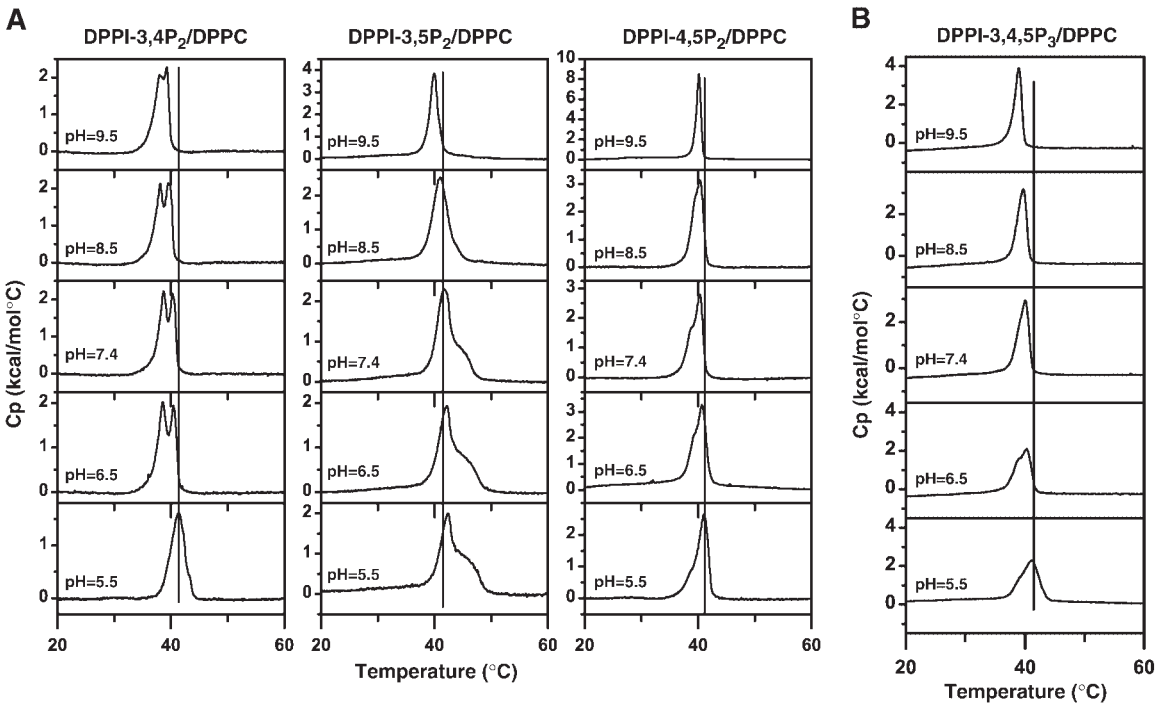

Fig. 2. A: Differential scanning calorimetry (DSC) thermograms of dipalmitoylphosphatidylinositol (DPPI)-x,y-P_2/dipalmitoylphosphatidylcholine (DPPC) (15:85) mixed multilamellar vesicles as a function of pH value. B: DSC thermograms of DPPI-3,4,5-P_3/DPPC (15:85) mixed multilamellar vesicles as a function of pH value. For both A and B, conditions were as follows: 0.3 mM total lipid concentration, third heating scan, heating rate of 0.5°C/min, buffer composition of 100 mM NaCl, 10 mM buffer, and 0.1 mM EDTA; see Materials). The line in each scan indicates the phase transition temperature of pure DPPC vesicles. Cp, heat capacity.

experiments. Although the DSC experiments were very useful for characterization of the thermotropic behavior of the PC-rich phase, it is not possible to extract more detailed information about the composition of the respective PI-PP phase (in other words, the extent of demixing), because a complete phase diagram cannot be obtained. To gain a better understanding of the phase behavior of phosphoinositide-rich phases, infrared transmission spectroscopy of mixed multilamellar phosphoinositide/perdeuterated PC vesicles was used.

Infrared spectroscopy

Lipid phase behavior can be studied with FTIR spectroscopy by monitoring the position of the methylene-stretching vibration bands, which have been shown to shift to higher wave numbers as the lipid acyl chains become more disordered (26, 27). In binary mixtures, the acyl chain order of individual lipids can be analyzed independently by using an acyl chain deuterated lipid as one of the two components (28). That is, the acyl chain order of the deuterated component can be studied based upon the antisymmetric CD_2 stretching vibration band [$\nu_a(CD_2)$], whereas the symmetric CH_2 stretching band [$\nu_s(CH_2)$] is used to monitor the nondeuterated lipid. As a result, the extent of lipid demixing (domain formation) can be analyzed by comparing the temperature-dependent behavior of the $\nu_a(CD_2)$ and the $\nu_s(CH_2)$ bands. For the purposes of this study, we used acyl chain deuterated DPPC-d_{62} as the deuterated component, which as a result of the isotopic labeling exhibits a slightly lower phase transition temperature than its nondeuterated analog (36.6°C instead of 41.3°C).

Figure 3A shows the $\nu_s(CH_2)$ and $\nu_a(CD_2)$ band frequencies of DPPI-x,y-P_2/DPPC-d_{62} (15:85) mixed multilamellar vesicles as a function of temperature. For all three DPPI-x,y-P_2 derivatives, a complex, pH-dependent mixing behavior with DPPC-d_{62} is observed. All investigated mixtures exhibit for the phosphoinositide component a broad phase transition above the phase transition temperature of the DPPC-d_{62} component. The observed demixing (i.e., domain formation) is generally most pronounced for pH levels of ~8.5; however, the detailed phase behavior of the mixtures is found to be strongly dependent on the phosphate substitution pattern at the inositol ring of the phosphoinositide component.

In the case of DPPI-3,4-P_2/DPPC-d_{62} mixed vesicles, the cooperativity (width of the transition range) as well as the temperatures of the DPPC-d_{62} main phase transition change only slightly as the pH is decreased (from 37.3°C at pH 9.5 to 39.5°C at pH 4.5). The increased phase transition temperature of the DPPC-d_{62} component at pH 4.5 (~2°C above the T_m of pure DPPC-d_{62}) suggests an enhanced mixing of the two lipid components, which should also be reflected in the phase behavior of the DPPI-3,4-P_2 component. This is indeed the case, because along with a broad transition centered at ~57°C, a second, smaller transition at ~40°C is discernible. As noted above, the transition peak found in the DSC thermograms is largely associated with the phase behavior of the DPPC component, which implies that the infrared results obtained for

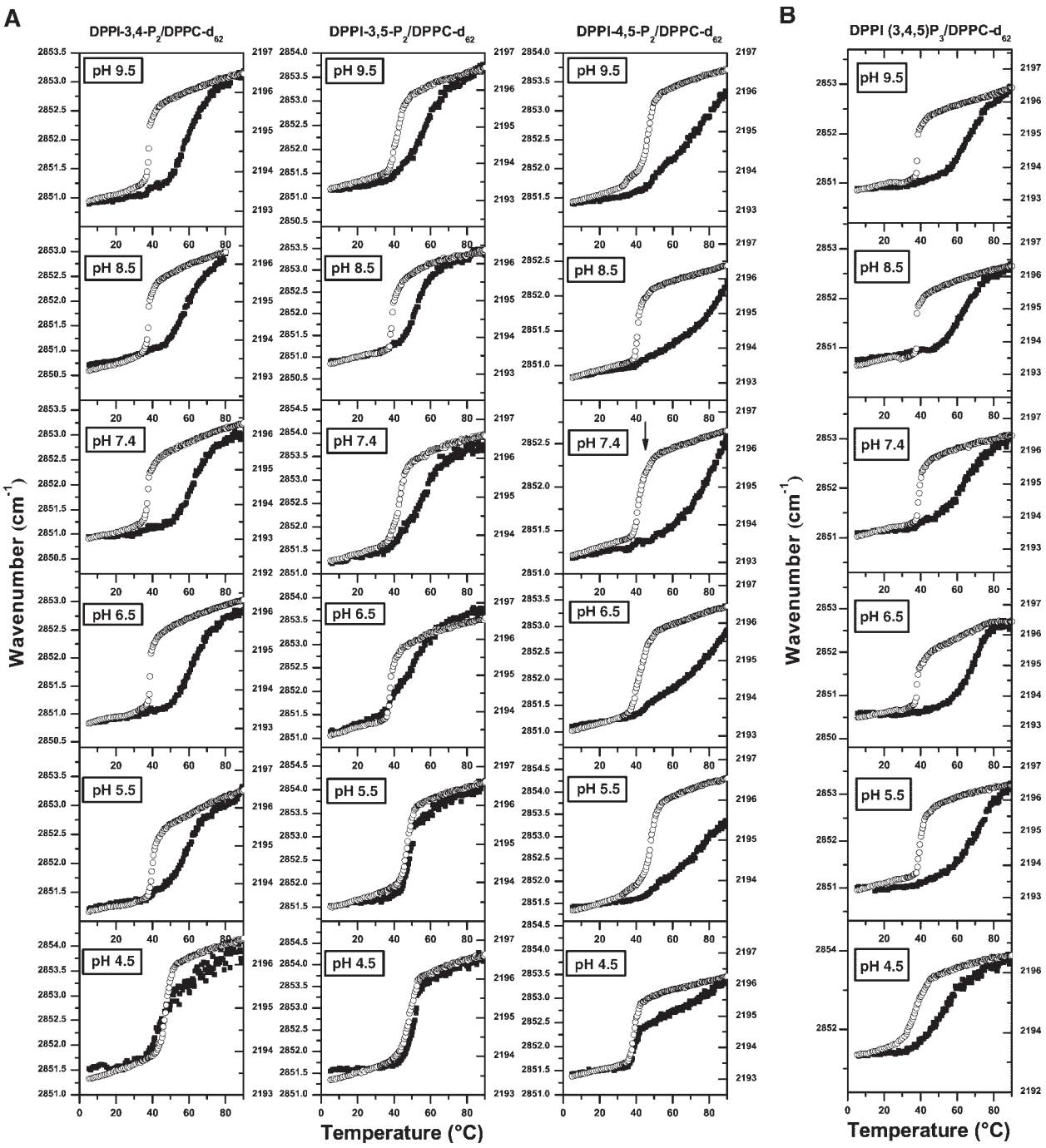

Fig. 3. A: Methylene-stretching band frequencies vs. temperature for DPPI-x,y-P_2/DPPC-d_{62} (15:85) mixed multilamellar vesicles at different pH values. Closed squares, symmetric CH_2 stretching band; [$\nu_s(CH_2)$] of DPPI-x,y-P_2 (left axis); open circles, antisymmetric CD_2 stretching vibration band [$\nu_a(CD_2)$] of DPPC-d_{62} (right axis). B: Methylene-stretching band frequencies vs. temperature for DPPI-3,4,5-P_3/DPPC-d_{62} (15:85) mixed multilamellar vesicles at different pH values. Closed squares, antisymmetric CH_2 stretching band [$\nu_s(CH_2)$] of DPPI-3,4,5-P_3 (left axis); open circles, $\nu_a(CD_2)$ of DPPC-d_{62} (right axis). Total experimental time was 36 h. Total lipid concentration was 40.6 mM. Buffer consisted of 100 mM NaCl, 10 mM buffer, and 0.1 mM EDTA (see Materials).

DPPC-d_{62} should be in general agreement with the phase behavior inferred from the DSC experiments. Because of the isotopic labeling, the DPPC phase transition temperature is lower than in the DSC experiment (36.6°C instead of 41.3°C); therefore, only the width and the relative temperature shift of the phase transitions can be compared between the DSC and infrared measurements. Taking this into consideration, the DSC and infrared experiments for PI-3,4-P_2/PC mixed vesicles agree well. For example, a broadened phase transition at an increased temperature is found for both types of experiment at pH 5.5 (compare Figs. 2A, 3A). The peak splitting observed in the DSC thermograms for pH levels between 6.5 and 8.5 is less obvious in the infrared experiments; however, a small fea-

ture (barely visible; see pH 7.4 and 6.5) discernible at the end of the DPPC-d_{62}-associated phase transition probably corresponds to the second transition found in the DSC plot. In this context, it is important to note that the DSC experiment is generally more efficient at resolving poorly separated phase transitions.

Similar to the DSC experiments, the infrared measurements reveal for DPPI-3,5-P_2/DPPC-d_{62} mixed vesicles a phase behavior that significantly deviates from the behavior found for the other phosphoinositides. The phase transition temperature of the DPPC-d_{62} component is for all investigated pH values above the T_m of pure DPPC-d_{62}, and the two lipids form at pH 5.5 a largely mixed phase with a T_m of ~48°C. Similar to the results obtained for the other lipid mixtures, the most pronounced demixing is observed at pH 8.5 (indicated by a DPPC-d_{62} phase transition temperature close to the T_m of the pure component). However, the corresponding PI-3,5-P_2 phase transition is found at a significantly lower temperature than was observed for PI-4,5-P_2 and PI-3,4-P_2. This implies that the stability of PI-3,5-P_2-enriched phases is reduced compared with the other PI-x,y-P_2 derivatives.

Arguably, DPPI-4,5-P_2/DPPC-d_{62} mixed vesicles show the most complex pH-dependent phase behavior. Although also in this case the most pronounced phase separation is found at pH 8.5, the increased temperature as well as the increased width of the DPPC-d_{62} phase transition is indicative of a less complete demixing than was observed for DPPI-3,4-P_2/DPPC-d_{62} mixed vesicles. At pH 7.4, the DPPC-d_{62} phase transition is found at a slightly higher temperature than at pH 8.5, and a small feature (marked by an arrow) is discernible at ~46°C. Upon further reduction of the pH, this "high"-temperature phase transition becomes dominant and only a minor subpopulation of the DPPC-d_{62} molecules is associated with the "low"-temperature phase transition (Fig. 3A, pH 5.5). For the DPPI-4,5-P_2 component, a very broad phase transition with an end point beyond the experimentally accessible temperature range is found. Upon decreasing the pH, the phase transition narrows and a second transition at ~45–46°C appears (i.e., concurrent with the DPPC-d_{62} phase transition). Similarly, at pH 9.5, the DPPC-d_{62} phase transition is shifted to higher temperatures and the DPPI-4,5-P_2 trace shows a small transition in that temperature region. It is important to emphasize that the data obtained for DPPI-4,5-P_2/DPPC-d_{62} mixed vesicles indicate only a partial demixing at pH 7.4.

In the case of DPPI-3,4,5-P_3/DPPC-d_{62} mixed vesicles (Fig. 3B), the phase transition of the DPPC-d_{62} component at pH 9.5 is found at a temperature close to the T_m of the pure lipid, and in accordance with the DSC measurements, the transition is quite narrow. The decrease of the pH value results in a slight high-temperature shift and a broadening of the DPPC-d_{62} transition region. For the DPPI-3,4,5-P_3 component, the phase transition is generally quite broad, and except for a slight narrowing, only minor changes in the DPPI-3,4,5-P_3 phase behavior are observed as the pH is decreased.

Comparison of the transition temperatures of the respective phosphoinositide-enriched phases reveals quite pronounced differences. Although for the DPPI-4,5-P_2/DPPC-d_{62} system the extent of demixing appears to be somewhat limited (see above), the corresponding DPPI-4,5-P_2-enriched phase is the most stable of all phosphoinositide-enriched domains. Although DPPI-3,4-P_2-enriched phases show a slightly higher stability than PI-xP phases (i.e., the phase transition is found at a higher temperature), the opposite is found for DPPI-3,5-P_2 (for the corresponding PI-xP data, see 23).

Physiological phosphoinositide concentrations are well below the 15% used for this study. To test for lipid demixing in a physiologically more relevant system, we investigated DPPI-4,5-P_2/DPPC-d_{62} (1:99) mixed vesicles by infrared spectroscopy and found essentially the same phase behavior that was observed for the mixed vesicles with higher DPPI-4,5-P_2 concentrations (data not shown).

In summary, the infrared data suggest gel phase demixing at ~pH 8.5 for all phosphoinositide/PC mixed vesicles. However, the extent of the demixing as well as the stability of the phosphoinositide-enriched phase is strongly dependent on the number and position of the respective phosphomonoester groups at the inositol ring (Fig. 3A, B). The lipid mixing improves as the pH is decreased, and for DPPI-x,y-P_2/DPPC-d_{62} mixed vesicles, a completely mixed state is obtained at pH 4.5. The question arises of whether the observed gel phase demixing manifests itself also in the physiologically more relevant fluid phase. Only limited information about this phase can be inferred from infrared spectroscopy measurements; therefore, a novel FRET assay was developed recently to enable the analysis of fluid/fluid demixing (23).

FRET measurements

Fluorescence quenching and FRET measurements have been used extensively to characterize domain formation in biological model membrane systems. Both techniques use fluorescently labeled molecules with a preference for either the domain or the surrounding phase. FRET measurements typically use two fluorescent probes, which enrich in environments with deviating physical properties. The FRET signal depends on the spectral properties of the donor and acceptor molecules, the proper alignment of the respective transition moments, and most importantly, the distance between the two labeled molecules (typically <10 nm), which enables the identification of colocalization (mixing) and separation (domain formation) of the probe molecules. The majority of FRET studies directed at the characterization of lipid domain formation have used probes with differential preferences for ordered or disordered environments. Although such a choice is appropriate for the characterization of raft domain formation (which is largely driven by interactions in the hydrophobic moiety), it is less suitable for the investigation of headgroup-driven domain formation. Therefore, we recently introduced a novel FRET assay that uses headgroup-specific chain-labeled PCs and chain-labeled phosphoinositides as probe molecules. From the point of view of chain composition, both labeled lipid molecules prefer to

enrich in the most fluid phase. These preferences are expected to be altered by strong interactions in the headgroup moiety, which should result in colocalization (domain formation) of headgroup-matched unlabeled and labeled lipid molecules (i.e., the labeled phosphoinositide molecules are expected to partition into phases rich in unlabeled phosphoinositide). As a result, the distance between the two types of labeled lipid molecules increases and a reduction of the resonance energy transfer occurs. To avoid transbilayer FRET as well as to enable convenient pH titration, the two probe molecules were fused into the outer leaflet of the bilayer by adding them as monomers to the preformed lipid vesicles (for more details, see 23). All experiments using saturated chain lipids were carried out at 70°C (i.e., well above the gel/liquid-crystalline phase transition temperature of both the PC and phosphoinositide components). In the case of the phosphoinositide lipids with natural chain composition (i.e., largely stearoyl/arachidonoyl), an experimental temperature of 20°C was used. In all cases, NBD was used as the donor and Bodipy was used as the acceptor fluorophores (see Materials).

Figure 4 shows the fluorescence spectra for DPPI-3,4-P_2/DPPC (15:85) mixed vesicles labeled with Bodipy-PI-3,4-P_2 (1.2 mol%) and NBD-PC (1.0 mol%) as a function of pH (70°C; i.e., fluid lipid phase). It can clearly be seen that the acceptor emission intensity is low at high pH and increases as the pH is decreased (i.e., at high pH, DPPI-3,4-P_2-rich domains are apparently formed). This pH-dependent domain formation was fully reversible (i.e., adjustment of the pH from 3 back to 10 resulted in the same transfer ratios as at the beginning of the experiment). The fluorophore concentrations used in the FRET experiments are quite high, and obviously fluorescence self-quenching needs to be considered. This self-quenching should be most pronounced in the case of phosphoinositide domain formation [i.e., this process will reduce the acceptor emission intensity even further than expected from the reduced resonance energy transfer (in other words, self-quenching amplifies the acceptor/emission ratio differences between the mixed and demixed states)]. **Figure 5A** displays the raw fluorescence emission spectra for the DPPI-x,y-P_2/DPPC and DPPI-3,4,5-P_3/DPPC mixtures at pH ~ 7.4, and Fig. 5B shows the acceptor/donor emission ratios for mixed vesicles composed of DPPI-3,4-P_2, DPPI-3,5-P_2, DPPI-4,5-P_2, or DPPI-3,4,5-P_3 and DPPC (15:85; all samples were labeled with NBD-PC and Bodipy-X, where X = PI-3,4-P_2, PI-3,5-P_2, PI-4,5-P_2, or PI-3,4,5-P_3).

Generally, the fluorescence intensities observed in the raw spectra showed a typical magnitude (Fig. 5A), which indicated that the monomeric labeled lipids inserted well into the preformed unilamellar vesicles (the NBD fluorophore is nonfluorescent in aqueous environments). In this regard, the DPPI-3,5-P_2/DPPC system was an exception because the fluorescence intensities were significantly lower, which suggests a reduced insertion of the labeled lipids. At present, we can only speculate about the reasons for the poor insertion, but fluorophore degradation was ruled out as a possible cause. Instead, the poor insertion appears to be linked to the physical properties of DPPI-3,5-P_2/DPPC mixed vesicles, which underscores the uniqueness of this system already highlighted by the infrared measurements.

For all DPPI-x,y-P_2/DPPC and DPPI-3,4,5-P_3/DPPC mixtures, the acceptor/donor emission ratios are small for high pH values, whereas for low pH values the ratios are significantly increased. Although DPPI-3,5-P_2/DPPC vesicles showed poor insertion of the labeled lipids (see above), resulting in reduced transfer ratios in the mixed state, the transfer ratio vs. pH trace is still similar to those traces obtained for the other phosphoinositides (i.e., at high pH, the transfer ratios are low and increase as the pH is decreased). With the exception of DPPI-4,5-P_2-containing vesicles, the transition from the demixed state (low ratio) to the mixed state (high ratio) occurs between pH ~7.4 and ~4.4 (midpoint is pH ~5.8–6.1) and was found to be fully reversible. The trace for DPPI-4,5-P_2/DPPC mixed vesicles shows, in contrast to all other investigated systems (including PI-xP-containing vesicles; see 23), an inflection between pH 7 and 8, which results in enhanced transfer ratios at physiological pH, indicating partial disintegration of DPPI-4,5-P_2-enriched domains at physiological pH.

Although the above experiments were conducted at a temperature that coincides with a fluid lipid state, the saturated chains of the lipid molecules might still aid the formation of phosphoinositide-enriched domains. To explore whether fluid/fluid demixing also occurs for available phosphoinositide/PC mixtures with natural chain compositions, the above experiments were repeated with bovine

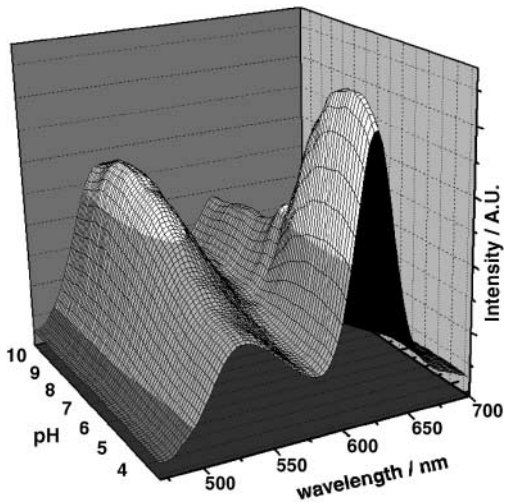

Fig. 4. Fluorescence spectra for DPPI-3,4-P_2/DPPC (15:85) mixed vesicles labeled with 1.2 mol% D(+)-*sn*-1-*O*-[1-[6′-[6-[((4-(4,4-difluoro-5-(2-thienyl)-4-bora-3a,4a-diaza-*s*-indacene-3-yl)phenoxy)acetyl)amino]hexanoyl]amino]hexanoyl]2-hexanoylglyceryl D-*myo*-phosphatidylinositol-3,4-bisphosphate (Bodipy-PI-3,4-P_2) and 1.0 mol% 1-palmitoyl-2-[12-[(7-nitro-2-1,3-benzoxadiazol-4-yl)amino]dodecanoyl]*sn*-glycero-3-phosphocholine (NBD-PC; 0.18 mM total lipid concentration, 70°C). Labeled lipids were fused into the outer leaflet of the preformed unilamellar vesicles. Lipid suspensions were titrated with 0.1 M HCl from pH 10 to 3.5 in steps of ~0.3. Buffer consisted of 100 mM NaCl, 10 mM HEPES, and 0.1 mM EDTA. A.U., arbitrary units.

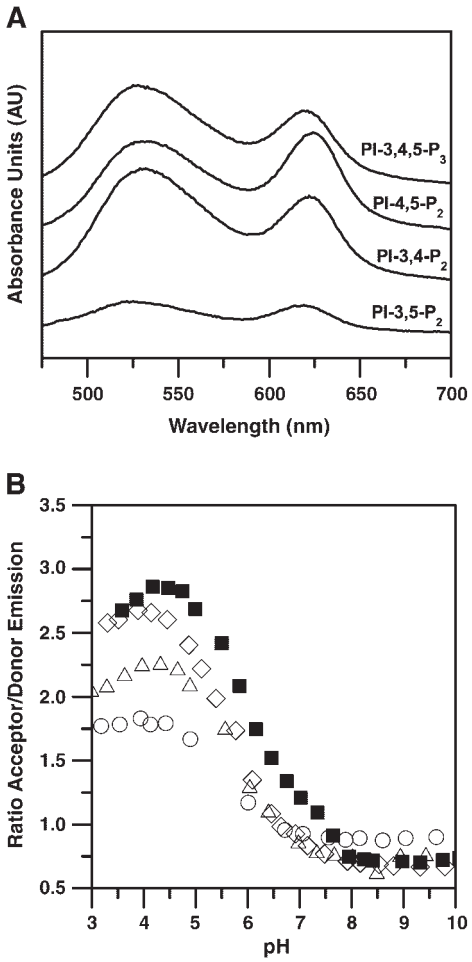

Fig. 5. A: Fluorescence spectra for DPPI-x,y-P_2/DPPC and DPPI-3,4,5-P_3/DPPC (15:85) mixed vesicles (pH ~ 7.4, 70°C, total lipid concentration 0.18 mM). Labeled NBD-PC (1.0 mol%) and Bodipy-PI-x,y,z-$P_{2\text{ or }3}$ (1.2 mol%) were fused into the outer leaflet of the preformed unilamellar vesicles. B: Corresponding ratios of the acceptor (~617 nm) and donor (~534 nm) emission intensities as a function of pH. Open diamonds, PI-3,4-P_2/PC; closed squares, PI-4,5-P_2/PC; open circles, PI-3,5-P_2/PC; open triangles, PI-3,4,5-P_3/PC. Buffer consisted of 100 mM NaCl, 10 mM HEPES, and 0.1 mM EDTA.

liver PI/POPC, brain PI-4P/POPC, brain PI-4,5-P_2/POPC (all natural phosphoinositides are rich in stearoyl at the *sn*-1 position and arachidonoyl at the *sn*-2 position), and SAPI-3,4,5-P_3/POPC mixtures (**Fig. 6**) at 20°C (fluid lipid state). In all cases, the data are in general agreement with the results obtained for the saturated chain analogs (i.e., at high pH, domain formation is observed, whereas reduction of the pH leads to an enhanced mixing of the respective two lipid components). However, in some instances, the exact pH dependence of the transfer ratio deviates slightly (e.g., the trace for the brain PI-4,5-P_2-containing vesicle is shifted with respect to the saturated chain analog to higher pH values, whereas the opposite is observed for SAPI-3,4,5-P_3). In conclusion, natural chain PI-4P and PI-3,4,5-P_3 form at physiological pH domains, whereas the domain-forming tendency of PI-4,5-P_2 is already slightly reduced at this pH. For all investigated natural chain PI-PP/PC mixtures, the demixing was most pronounced at approximately pH 8.5, whereas the PI-PP-enriched domains disintegrate at low pH.

As noted above, physiological concentrations of phosphatidylinositol bisphosphates are considerably lower than the concentrations used above (e.g., typical PI-4,5-P_2 plasma membrane concentrations are in the range of 1%). To test the extent of domain formation for these PI-4,5-P_2 levels, FRET experiments were conducted for 99% PC and 1% PI-4,5-P_2 (in both cases including labeled lipids) (**Fig. 7**). Although the transfer ratio difference between the mixed and demixed states is reduced compared with the results obtained for the mixed vesicles with higher PI-4,5-P_2 concentrations (most likely because of the unfavorably low ratio of unlabeled to labeled PI-4,5-P_2), the mixture remains largely demixed at pH $\geq$ 8.5 and shows enhanced mixing as the pH is decreased. It is worth mentioning that measurements for 1% PI-4P/99% POPC also gave results in agreement with those obtained for mixed vesicles containing 15% PI-4P (23).

DISCUSSION

The experiments described here aimed to investigate the extent of phosphoinositide domain formation and were designed to explore whether the phosphate substitution pattern at the inositol ring influences the mutual phosphoinositide interaction. The project was driven by the hypothesis that the bilayer structure in the vicinity of phosphoinositides is not only governed by the number but also by the position of the respective phosphomonoester groups at the inositol ring.

This study as well as an earlier one on PI-xPs (23) gave results consistent with the formation of phosphoinositide-enriched domains at or above physiological pH. The Pk_{a2} values for micellar PI-4P and PI-4,5-P_2 were reported to be 6.5–7.6 (depending on the position of the phosphomonoester group at the inositol ring), which implies that the maximum mutual phosphoinositide interaction is found in a pH range leading to a predominantly deprotonated phosphomonoester group. This observation is in contrast to the results obtained for PA, in which a stabilization of the gel phase was found for pH values between the Pk_{a1} and Pk_{a2} of the phosphomonoester group (29). In that case, it was rationalized that the enhanced mutual PA interaction is attributable to the formation of a hydrogen bond network between adjacent phosphomonoester groups, which function as a proton donor as well as a proton acceptor. In light of the pH dependence of the mutual phosphoinositide interaction, it can be ruled out that such a mechanism is a contributing factor to the observed stabilization of phosphoinositide-enriched domains because the largely deprotonated phosphomonoester groups (pH > Pk_{a2}) cannot donate a hydrogen atom for the formation of a hydrogen bond network. Furthermore, the deprotonation of the phosphomonoester groups results in a high charge of the respective phosphoinositide headgroup, which should lead to strong repulsive forces and, therefore, enhanced phosphoinositide/PC mixing at high pH. How-

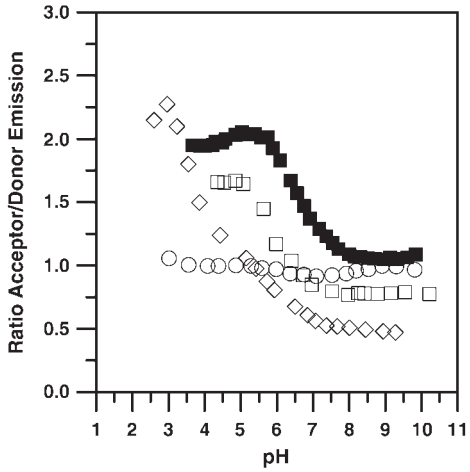

Fig. 6. Ratios of the acceptor (~617 nm) and donor (~534 nm) emission intensities as a function of pH for bovine liver PI/palmitoyloleoylphosphatidylcholine (POPC), brain PI-4P/POPC, brain PI-4,5-P_2/POPC, and stearoylarachidonoylphosphatidylinositol-3,4,5-trisphosphate (SAPI-3,4,5-P_3)/POPC (15:85) (total lipid concentration 0.18 mM, 20°C). Labeled NBD-PC (1.0 mol%) and Bodipy-PI or Bodipy-PI-x,y,z-$P_{2\text{ or }3}$ (1.2 mol%) were fused into the outer leaflet of the preformed unilamellar vesicles. Open circles, PI /PC; closed squares, PI-4,5-P_2/PC; open squares, PI-4P/PC; open diamonds, PI-3,4,5-P_3/PC. Buffer consisted of 100 mM NaCl, 10 mM HEPES, and 0.1 mM EDTA.

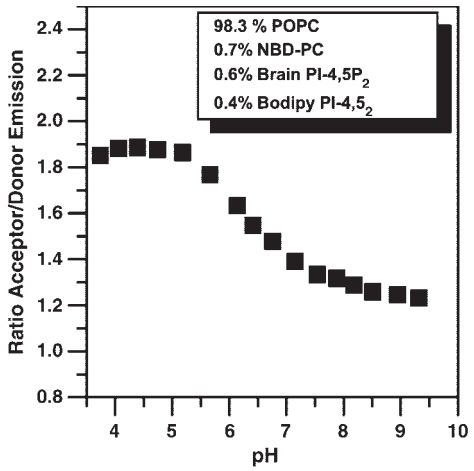

Fig. 7. Ratios of the acceptor (~617 nm) and donor (~534 nm) emission intensities as a function of pH for brain PI-4,5-P_2/POPC (0.6%/98.3%) (total lipid concentration 0.18 mM, 20°C). Labeled NBD-PC (0.7 mol%) and Bodipy-PI-4,5-P_2 (0.4 mol%) were fused into the outer leaflet of the preformed unilamellar vesicles. Closed squares, PI-4,5-P_2/POPC. Buffer consisted of 100 mM NaCl, 10 mM HEPES, and 0.1 mM EDTA.

ever, the opposite is observed, which suggests that these unfavorable repulsive forces are overcome by attractive forces, most likely involving hydroxyl/hydroxyl, hydroxyl/phosphodiester, and hydroxyl/phosphomonoester interactions.

The phase behavior of phosphoinositide/PC mixed vesicles also departs for slightly acidic pH values from the phase characteristics established for PA/PC mixtures (30). In the case of PA/PC, an enhanced demixing was observed for this pH range, which was attributed to the aforementioned formation of a hydrogen bond network. In contrast, phosphoinositide/PC mixtures exhibit enhanced mixing for pH values <7, which implies that also for these pH values phosphomonoester group interactions between adjacent phosphoinositide headgroups are not a contributing factor for the stabilization of phosphoinositide-enriched regions of the bilayer. Furthermore, in the case of DPPI-4,5-P_2- and DPPI-3,5-P_2-containing mixtures, the phase transition temperatures of the DPPC-d_{62} component shift significantly to higher temperatures (Fig. 3A), indicating nonideal mixing characterized by attractive forces between unlike molecules. It is important to note that PC was chosen for this study because this lipid provides a more stabile and reproducible environment for phosphoinositides than phosphatidylethanolamine or phosphatidylserine. Furthermore, the physiological importance of phosphoinositides is not restricted to the plasma membrane, and phosphoinositides are found in varying lipid environments. The primary goal of this study was to highlight the mutual interaction of phosphoinositides, and in this context, the primary function of PC is to serve as a matrix.

PI-PP/PC vesicles showed, compared with PI-xP-containing vesicles (23), an increased extent of demixing as well as an enhanced stability of phosphoinositide-enriched domains. Furthermore, PI-x,y-P_2/PC mixed vesicles exhibited a more pronounced phosphate substitution pattern dependent on the variability of the physical properties of phosphoinositide-enriched bilayer regions. It is important to stress that the position of the phosphomonoester groups at the inositol ring not only influences the extent of domain formation as well as domain stability at high pH but also affects the PI-PP/PC interaction in the mixed state (low pH; see discussion for PI-3,5-P_2 below). The mutual interaction of phosphoinositides is expected to depend on a proper orientation of the hydroxyl and phosphate groups with respect to each other; therefore, it is not surprising that the positions of the respective phosphomonoester groups at the inositol ring are of importance for the observed domain formation. In this context, it is worth mentioning that recent molecular dynamics calculations showed that PI-4,5-P_2 in a mixture with dimyristoylphosphatidylcholine (DMPC) forms clusters that are stabilized by bridging water molecules between hydroxyl and phosphate groups of adjacent PI-4,5-P_2 headgroups (31).

PI-4,5-P_2/PC mixed vesicles

The infrared transmission experiments revealed DPPI-4,5-P_2 gel phase domain formation at approximately pH 8.5; similarly, the results obtained from the FRET measurements suggest the formation of "fluid-type" domains at the same pH. This fluid/fluid demixing (FRET experiment) was observed for PI-4,5-P_2/PC mixtures with different chain compositions (saturated chains at 70°C vs. natural chain composition at 20°C) and PI-4,5-P_2 concentrations as low as 1%. What sets PI-4,5-P_2 apart from the other phosphoinositides is the significantly reduced domain-forming ten-

dency at physiological pH (i.e., at approximately pH 7, enhanced PI-4,5-P_2/PC mixing is observed). For micellar PI-4,5-P_2, the phosphate group at the 4′ position exhibited a Pk_{a2} of 6.7, whereas for the phosphate group at the 5′ position, a Pk_{a2} of 7.6 was found (32). It is worth mentioning that the small but reproducible inflection found in the trace of the PI-4,5-P_2/PC FRET experiments is localized around the Pk_{a2} of the 5′ phosphate group, whereas the beginning of the steeper part of the trace coincides with the Pk_{a2} of the phosphate group at the 4′ position. Similar to all other phosphoinositides, maximum domain formation is found at a pH above the Pk_{a2} of the phosphomonoester groups (i.e., the majority of the phosphomonoester groups are deprotonated when the strongest mutual phosphoinositide interaction is found).

Generally, the pH dependence of PI-4,5-P_2/PC demixing is conserved for all investigated systems; in other words, the results obtained for DPPI-4,5-P_2/DPPC-d_{62} in the gel phase, DPPI-4,5-P_2/DPPC in the fluid phase, and brain PI-4,5-P_2/POPC in the fluid phase were all consistent with a demixed state at high pH. However, a more detailed comparison of these three systems exposes some differences. The most ordered system, DPPI-4,5-P_2/DPPC-d_{62} in the gel phase, appears to be slightly more demixed between pH 6 and 7 than was found for the mixtures in the fluid phase. Furthermore, comparison of the FRET results obtained for DPPI-4,5-P_2/DPPC mixtures at 70°C and for brain PI-4,5-P_2/POPC mixtures at 20°C reveals a minute shift of the demixed/mixed transition to higher pH for the natural chain lipid composition. These results might indicate that a tighter packing of the lipids enhances the mutual phosphoinositide headgroup interaction, which would result in increased stabilization of the respective phosphoinositide-enriched domains.

PI-3,5-P_2/PC mixed vesicles

Among all PI-PPs, the gel phase demixing is the least pronounced for DPPI-3,5-P_2-containing mixed vesicles. Furthermore, the pronounced high-temperature shift of the DPPC-d_{62} transition temperature at pH 4.5 and 5.5 indicates a quite strong DPPI-3,5-P_2/DPPC interaction, which is also evident in the DSC thermograms (pronounced high-temperature shoulder). The results from the FRET experiment are inconclusive because of the poor insertion of the labeled lipids. At present, we can only speculate regarding this behavior, but it appears that the lack of labeled lipid insertion is linked to the unique physical state of DPPI-3,5-P_2/DPPC vesicles.

PI-3,4-P_2/PC mixed vesicles

The results obtained from the infrared as well as the FRET measurements are consistent with DPPI-3,4-P_2 domain formation at or above physiological pH. The DPPI-3,4-P_2 data resemble those obtained for PI-xPs and deviate from the results found for the other two phosphatidylinositol bisphosphate derivatives (PI-4,5-P_2 and PI-3,5-P_2). For example, as the pH is decreased, the T_m of DPPC-d_{62} shifts significantly to higher temperatures for DPPI-4,5-P_2- and DPPI-3,5-P_2-containing vesicles. In the case of DPPI-3,4-P_2, the shift is minute (Fig. 3A), which suggests that the DPPI-3,4-P_2/DPPC interaction is only minor. Furthermore, the apparent disintegration of PI-3,4-P_2-enriched domains occurs at a slightly lower pH than is found for PI-4,5-P_2-enriched domains.

PI-3,4,5-P_3/PC mixed vesicles

At first glance, the phase behavior of PI-3,4,5-P_3/PC mixed vesicles is similar to that of PI-3,4-P_2/PC vesicles [i.e., the pH dependence of the PI-3,4,5-P_3 domain formation (FRET experiments) as well as the limited PI-3,4,5-P_3/PC interaction at pH 4.5 (infrared measurements) mirrors the conditions found for PI-3,4-P_2]. However, a more detailed inspection of the data reveals that the PI-3,4,5-P_3 gel phase is significantly more stable than the corresponding PI-3,4-P_2 phase. It is important to highlight that natural chain PI-3,4,5-P_3 domains remain intact to pH values significantly below physiological pH (FRET experiments; Fig. 6), which suggests that at physiological pH, PI-3,4,5-P_3-enriched domains are quite stable.

CONCLUSIONS

Biological membranes obviously contain a multitude of molecular species that affect the formation of phosphoinositide-enriched membrane regions in vivo; however, it is intriguing that PI-PPs exhibit a significant mutual interaction at physiological pH. However, the most abundant phosphoinositide, PI-4,5-P_2, shows a slightly reduced domain-forming tendency at physiological pH compared with the other phosphoinositide derivatives. This reduced domain tendency might suggest that PI-4,5-P_2 segregation requires the presence of other chemical species (e.g., basic proteins or bivalent cations). 3′ phosphorylated phosphoinositides are far less abundant than PI-4,5-P_2, and their accumulation is believed to be transient and locally restricted. In this context, the stronger mutual interaction of PI-3-P, PI-3,4-P_2, and PI-3,4,5-P_3 at physiological pH potentially aids local enrichment and might stabilize such regions for sufficiently long periods for proteins to interact.

The results presented here suggest that phosphoinositide-enriched domains are stabilized by a hydrogen bond network formed between the hydroxyl groups and the phosphomonoester as well as phosphodiester groups of adjacent molecules. Obviously, these interactions will depend on the geometry of the inositol phosphate headgroup; therefore, it is not surprising that these interactions depend not only on the number but also on the position of the phosphomonoester groups at the inositol ring. On the other hand, it is expected that these interactions will also lead to different headgroup orientations, which might affect the interaction of these lipids with phosphoinositide binding proteins.

The results presented in this paper highlight the general importance of hydrogen bond formation for the mutual interactions of phosphoinositides. Further experiments are needed to judge to what extent these interactions contribute in vivo to the local enrichment of phosphoinositides.

The help of Andrea N. Todaro and Stephan M. Woods in acquiring some of the FRET data is gratefully acknowledged. This research was funded by grants from the National Institutes of Health (R01-AR-038910) and the Ohio Board of Regents.

REFERENCES

1. Payrastre, B., K. Missy, S. Giuriato, S. Bodin, M. Plantavid, and M. P. Gratacap. 2001. Phosphoinositides—key players in cell signalling, in time and space. *Cell. Signal.* **13:** 377–387.
2. Stenmark, H., and D. J. Gillooly. 2001. Intracellular trafficking and turnover of phosphatidylinositol 3-phosphate. *Semin. Cell Dev. Biol.* **12:** 193–199.
3. Vanhaesebroeck, B., S. J. Leevers, K. Ahmadi, J. Timms, R. Katso, P. C. Driscoll, R. Woscholski, P. J. Parker, and M. D. Waterfield. 2001. Synthesis and function of 3-phosphorylated inositol lipids. *Annu. Rev. Biochem.* **70:** 535–602.
4. Wang, Y. J., J. Wang, H. Q. Sun, M. Martinez, Y. X. Sun, E. Macia, T. Kirchhausen, J. P. Albanesi, M. G. Roth, and H. L. Yin. 2003. Phosphatidylinositol 4 phosphate regulates targeting of clathrin adaptor AP-1 complexes to the Golgi. *Cell.* **114:** 299–310.
5. Carricaburu, V., K. A. Lamia, E. Lo, L. Favereaux, B. Payrastre, L. C. Cantley, and L. E. Rameh. 2003. The phosphatidylinositol (PI)-5-phosphate 4-kinase type II enzyme controls insulin signaling by regulating PI-3,4,5-trisphosphate degradation. *Proc. Natl. Acad. Sci. USA.* **100:** 9867–9872.
6. Padron, D., Y. J. Wang, M. Yamamoto, H. Yin, and M. G. Roth. 2003. Phosphatidylinositol phosphate 5-kinase I beta recruits AP-2 to the plasma membrane and regulates rates of constitutive endocytosis. *J. Cell Biol.* **162:** 693–701.
7. Bodin, S., S. Giuriato, J. Ragab, B. M. Humbel, C. Viala, C. Vieu, H. Chap, and B. Payrastre. 2001. Production of phosphatidylinositol 3,4,5-trisphosphate and phosphatidic acid in platelet rafts: evidence for a critical role of cholesterol-enriched domains in human platelet activation. *Biochemistry.* **40:** 15290–15299.
8. Caroni, P. 2001. Actin cytoskeleton regulation through modulation of PI(4,5)P-2 rafts. *EMBO J.* **20:** 4332–4336.
9. Hill, M. M., J. H. Feng, and B. A. Hemmings. 2002. Identification of a plasma membrane raft-associated PKB Ser473 kinase activity that is distinct from ILK and PDK1. *Curr. Biol.* **12:** 1251–1255.
10. Rozelle, A. L., L. M. Machesky, M. Yamamoto, M. H. E. Driessens, R. H. Insall, M. G. Roth, K. Luby-Phelps, G. Marriott, A. Hall, and H. L. Yin. 2000. Phosphatidylinositol 4,5-bisphosphate induces actin-based movement of raft-enriched vesicles through WASP-Arp2/3. *Curr. Biol.* **10:** 311–320.
11. Zhuang, L. Y., J. Q. Lin, M. L. Lu, K. R. Solomon, and M. R. Freeman. 2002. Cholesterol-rich lipid rafts mediate Akt-regulated survival in prostate cancer cells. *Cancer Res.* **62:** 2227–2231.
12. Partovian, C., and M. Simons. 2004. Regulation of protein kinase B/Akt activity and Ser^{473} phosphorylation by protein kinase Cα in endothelial cells. *Cell. Signal.* **16:** 951–957.
13. Parmryd, I., J. Adler, R. Patel, and A. I. Magee. 2003. Imaging metabolism of phosphatidylinositol 4,5-bisphosphate in T-cell GM1-enriched domains containing Ras proteins. *Exp. Cell Res.* **285:** 27–38.
14. Botelho, R. J., M. Teruel, R. Dierckman, R. Anderson, A. Wells, J. D. York, T. Meyer, and S. Grinstein. 2000. Localized biphasic changes in phosphatidylinositol-4,5- bisphosphate at sites of phagocytosis. *J. Cell Biol.* **151:** 1353–1367.
15. Marshall, J. G., J. W. Booth, V. Stambolic, T. Mak, T. Balla, A. D. Schreiber, T. Meyer, and S. Grinstein. 2001. Restricted accumulation of phosphatidylinositol 3-kinase products in a plasmalemmal subdomain during Fc gamma receptor-mediated phagocytosis. *J. Cell Biol.* **153:** 1369–1380.
16. Miaczynska, M., and M. Zerial. 2002. Mosaic organization of the endocytic pathway. *Exp. Cell Res.* **272:** 8–14.
17. Gillooly, D. J., C. Raiborg, and H. Stenmark. 2003. Phosphatidylinositol 3-phosphate is found in microdomains of early endosomes. *Histochem. Cell Biol.* **120:** 445–453.
18. Gambhir, A., G. Hangyas-Mihalyne, I. Zaitseva, D. S. Cafiso, J. Wang, D. Murray, S. N. Pentyala, S. O. Smith, and S. McLaughlin. 2004. Electrostatic sequestration of PIP2 on phospholipid membranes by basic/aromatic regions of the proteins. *Biophys. J.* **86:** 2188–2207.
19. Bodin, S., H. Tronchere, and B. Payrastre. 2003. Lipid rafts as critical membrane domains in blood platelet activation processes. *Biochim. Biophys. Acta.* **1610:** 247–257.
20. Magee, T., N. Pirinen, J. Adler, S. N. Pagakis, and I. Parmryd. 2002. Lipid rafts: cell surface signaling platforms for T-cell signaling. *Biol. Res.* **35:** 127–131.
21. Wanaski, S. P., B. K. Ng, and M. Glaser. 2003. Caveolin scaffolding region and the membrane binding region of src form lateral membrane domains. *Biochemistry.* **42:** 42–56.
22. Epand, R. M., P. Vuong, C. M. Yip, S. Maekawa, and R. F. Epand. 2004. Cholesterol dependent partitioning of PtdIns(4,5)P_2 into membrane domains by the N-terminal fragment of NAP-22 (neuronal axonal myristoylated membrane protein of 22 kDa). *Biochem. J.* **379:** 527–532.
23. Redfern, D. A., and A. Gericke. 2004. Domain formation in phosphatidylinositol monophosphate/phosphatidylcholine mixed vesicles. *Biophys. J.* **86:** 2980–2992.
24. Takizawa, T., Y. Nakata, A. Takahashi, M. Hirai, S. Yabuki, and K. Hayashi. 1998. Differential scanning calorimetry and ^{1}H-NMR study of aqueous dispersions of the mixtures of dipalmitoylphosphatidylcholine and phosphatidylinositol-4,5-bis(phosphate). *Thermochim. Acta.* **308:** 101–107.
25. Leidy, G., W. F. Wolkers, K. Jorgensen, O. G. Mouritsen, and J. H. Crowe. 2001. Lateral organization and domain formation in a two-component lipid membrane system. *Biophys. J.* **80:** 1819–1828.
26. McElhaney, R. N., and R. N. A. H. Lewis. 1995. Fourier transform infrared spectroscopy in the study of hydrated lipids and lipid bilayer membranes. *In* Infrared Spectroscopy of Biomolecules. H. H. Mantsch and D. Chapman, editors. Wiley, New York. 159–202.
27. Mendelsohn, R., and R. G. Snyder. 1996. Infrared spectroscopic determination of conformational disorder and microphase separation in phospholipid acyl chains. *In* Biological Membranes. K. M. Merz and B. Roux, editors. Birkhäuser, Boston. 145–174.
28. Mendelsohn, R., and D. J. Moore. 1998. Vibrational spectroscopic studies of lipid domains in biomembranes and model systems. *Chem. Phys. Lipids.* **96:** 141–157.
29. Eibl, H. 1983. The effect of the proton and of monovalent cations on membrane fluidity. *In* Membrane Fluidity in Biology. R. C. Aloia, editor. Academic Press, New York. 217–236.
30. Garidel, P., C. Johann, and A. Blume. 1997. Nonideal mixing and phase separation in phosphatidylcholine phosphatidic acid mixtures as a function of acyl chain length and pH. *Biophys. J.* **72:** 2196–2210.
31. van Paridon, P. A., B. de Kruijff, R. Ouwerkerk, and K. W. A. Wirtz. 1986. Polyphosphoinositides undergo charge neutralization in the physiological pH range: a ^{31}P-NMR study. *Biochim. Biophys. Acta.* **877:** 216–219.
32. Liepina, I., C. Czaplewski, P. Janmey, and A. Liwo. 2003. Molecular dynamics study of a gelsolin-derived peptide binding to a lipid bilayer containing phosphatidylinositol 4,5-bisphosphate. *Biopolymers.* **71:** 49–70.